

Silicon nanowire optical Raman line shapes at cryogenic and elevated temperatures

H. Scheel^{1,*}, S. Khachadorian¹, M. Cantoro², A. Colli², A. C. Ferrari², and C. Thomsen¹

¹ Institut für Festkörperphysik, Technische Universität Berlin, Berlin, Germany

² Department of Engineering, University of Cambridge, Cambridge CB3 0FA, UK

Received 7 May 2008, revised 18 July 2008, accepted 7 August 2008

Published online 10 September 2008

PACS 78.30.-j, 78.67.Lt

* Corresponding author: e-mail harald.scheel@tu-berlin.de

We report the Raman spectra of silicon nanowires (SiNWs) in a wide temperature range, between 2 K and 850 K. At room temperature we find a strong influence on the spectrum from applied laser excitation powers. These effects can be attributed to a laser heated sample, leading to an inhomogeneous temperature distribution within the laser-spot. If the laser excitation power is small (below 100 μW) such effects are negligible, and we find a temperature dependence governed by three-

phonon decay processes. The results from temperature dependent measurements indicate a change of sample morphology due to heating. Raman measurements on SiNWs immersed in superfluid helium at ≈ 2 K show very strong red-shifts, even though they still have the perfect thermal contact via the superfluid helium. Considering anharmonic effects we find massively increased Si core temperatures.

© 2008 WILEY-VCH Verlag GmbH & Co. KGaA, Weinheim

1 Introduction Nanometer sized semiconductor structures have attracted large attention. Two, one or zero-dimensional structures show very unique low-dimensional properties, leading to enhanced device performances. The research on carbon nanostructures like nanotubes [1] or nano-ribbons [2] is continuously generating an impressive variety of publications. The basic material of present information technology, however, is still silicon. While silicon structures have been intensively investigated for some time now, silicon nanowires (SiNWs) still face the lack of standard, non-destructive methods for their characterization.

Here we report the large Raman shift and broadening of the LO vibrational mode, due to a combination of quantum confinement and laser heating [4]. Our detailed analysis of the Raman spectrum of SiNWs and its dependence on the laser excitation power and sample temperature provides valuable information about the predominant effects in SiNW samples, while the strong influence of the ambience on SiNWs, as published elsewhere [5], needs to be suppressed to identify the effects intrinsic to SiNWs.

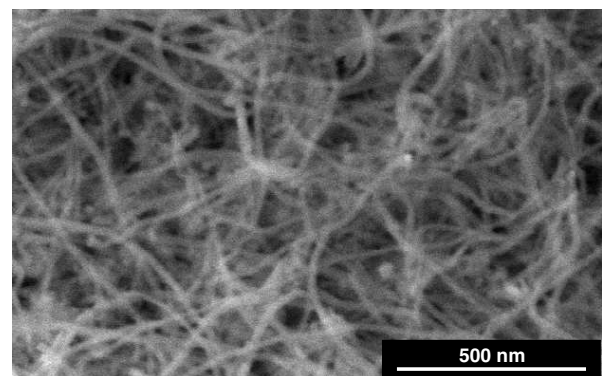


Figure 1 Typical SEM picture of SiNWs sample. The SiNW are approximately 15 nm in diameter and up to a few microns long. The sample consists of a large pile of SiNWs (up to 50 μm thick), showing a strong porosity.

2 Experimental The SiNWs used for this study were produced by vapor transport growth [6], which allows

high-yield SiNWs production. Si/SiO₂ powders are evaporated at 1200 °C in a horizontal tube furnace. The Si vapor then condenses at ≈ 800 °C on a substrate (average production ≈ 10 mg per run). The average wire diameter is 15 nm, consisting of an outer SiO₂ shell of 2-3 nm, and a crystalline core [6,7]. For Raman measurements the SiNWs are sonicated in isopropanol and dispersed on Ag coated Cu substrates. The SiNW sample-spots created by this procedure are one to two mm in diameter and approximately 20-50 μm thick, as observed by atomic force microscopy. Within the SiNW spot the wires are randomly arranged, this can be clearly seen in Fig. 1, which shows a scanning electron microscopy (SEM) image of wires, several microns in length. These are in contact to other wires, but well separated from the substrate. A cryostat sample chamber was flushed with He, air, or Ne to measure the SiNWs in different gases; we also performed low temperature measurements in superfluid He.

Macro-Raman spectra were excited with the 514 nm line of an Ar-ion laser, dispersed by a Dilor-XY800 Raman spectrometer, and detected with a charge coupled device. The exciting laser power P was measured in front of the cryostat window; 25% laser power is lost at the windows. The temperature dependent measurements were performed using a heating stage (LINKAM THMS 600). The nanowire Raman spectra were fitted by a Lorentzian for the main Raman feature plus a Gaussian for the low-energy tail, possibly related to amorphous silicon [8,9,4]. For our samples with an average diameter of 9 nm, phonon frequency shifts $\Delta\omega$ were determined with respect to the TO of a reference bulk Si sample, measured under the same experimental conditions. Note that our laser power densities are one to two orders of magnitude smaller than in previous Raman studies [4] because of the larger laser spot (~ 10 μm) in the macro-Raman setup.

3 Results and discussion All SiNW Raman spectra in this study are red-shifted compared to bulk Si. This is shown in Fig. 2, where the black and red spectrum represent bulk Si and SiNWs, respectively. Both spectra were recorded under the same conditions with moderate laser excitation powers (see legend). For higher laser powers (above 4-5 mW) we also observe [3,4] asymmetric line-shapes, where the asymmetry and amount of red-shift increase with laser power. For large excitation powers the red-shifting finally saturates, as reported earlier (see for example Fig. 3 in Ref. [5]). The maximum red-shift observed there was approximately 12 cm^{-1} , at room temperature irrespective of the ambient gas (He or Air). The critical laser excitation power (P_c), above which the saturation occurs, on the other hand strongly depends on the gas i.e. its thermal conductivity.

As reported earlier [10], inhomogeneous temperature profiles due to excessive laser heating, can lead to asymmetrically broadened Raman-spectra. In order to reduce effects related to the intensity profile of the laser spot

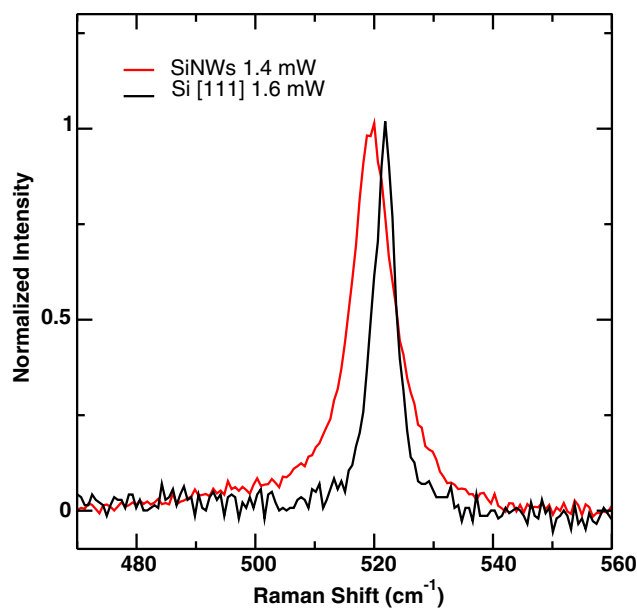


Figure 2 Typical room temperature Raman spectrum of our SiNW sample, illuminated by a moderate laser power of 1.4 mW (red line). For comparison we also plot a bulk silicon reference sample (black line).

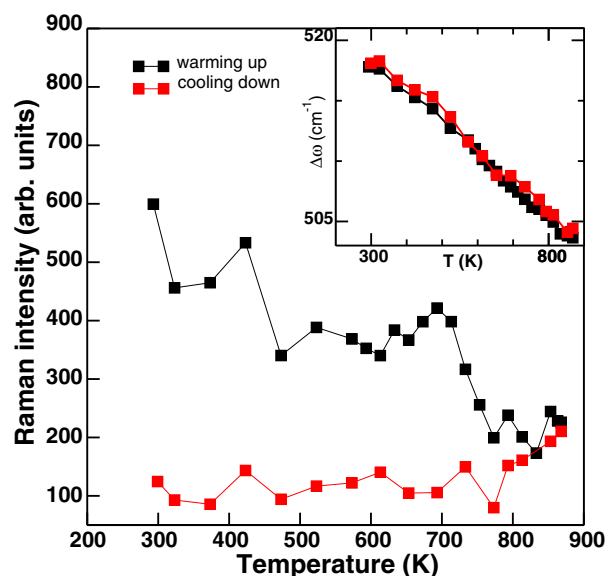


Figure 3 Raman intensity of SiNWs in air versus heating stage temperature for increasing (black squares) and decreasing (red squares) temperature. The inset shows the phonon frequencies of the same spectra. Both of the measurements are carried out with the laser power of ≈ 1 mW.

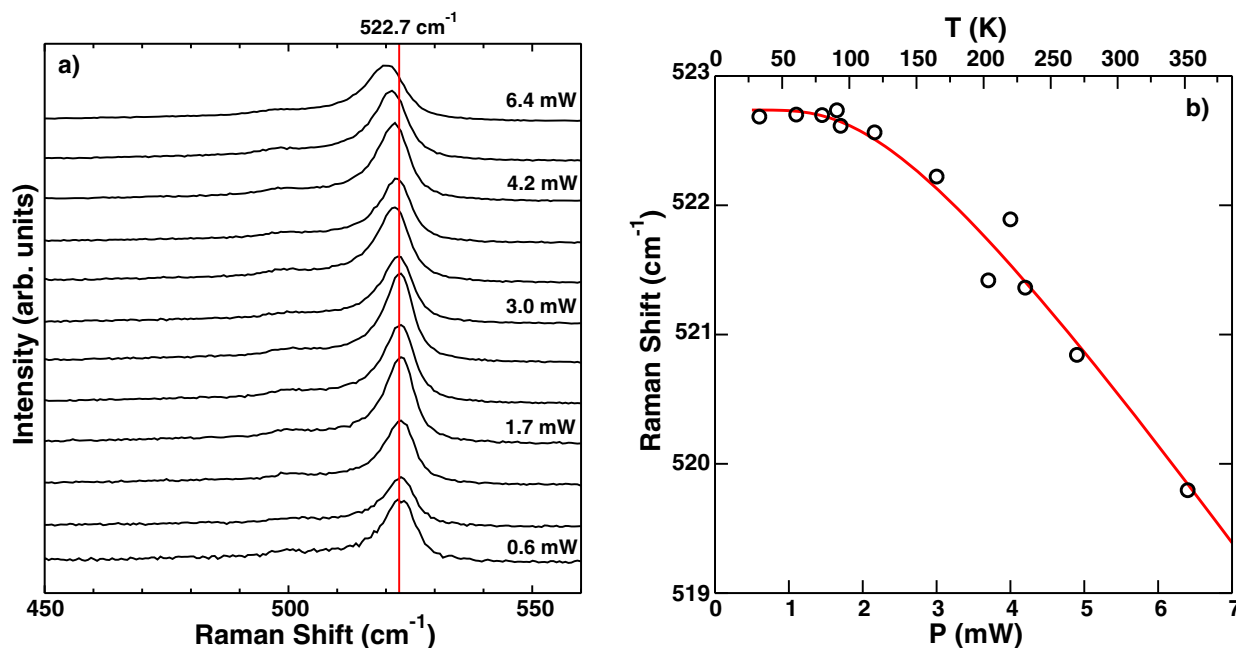


Figure 4 a) SiNW Raman spectra for different laser excitation powers, immersed in superfluid He. The laser powers are indicated for selected spectra. All spectra except for the 0.6 mW spectrum were shifted to allow for a better view. In b) the Raman peak positions from a) are plotted versus laser excitation power.

(*i.e.* the local, inhomogeneous temperatures) we further investigated the effect of saturation using a homogeneous temperature profile of a heating stage. The results are shown in the inset of Fig. 3, where we plot the SiNW phonon frequency as a function of heating stage temperature in air, under increasing (black squares) and decreasing temperatures (red squares). We observe an almost linear dependence, as expected from anharmonic theory [11,12]. Clearly, the heating and cooling process is reversible concerning the peak position, and no saturation in the frequency-temperature diagram is detected. The maximum red-shifts realized in the heating stage experiments ($\approx 14 \text{ cm}^{-1}$) are well above the maximum red-shifts observed in the laser-heated experiments of Ref. [5] ($\approx 12 \text{ cm}^{-1}$).

However, the high temperatures do have an effect on the sample. Figure 3 shows the Raman intensity versus SiNW sample temperature. Under increasing temperature we observe a gradual decline of the Raman intensity, induced by the intense heating. Cooling down the sample again the intensity stays nearly constant. Our measurements could be interpreted as if the morphology of the SiNW sample changes due to the heating processes, *i.e.* the sample surface is effectively lowered, moving out of the focal position of the laser spot. This results in a reduction of the Raman intensity as observed in Fig. 3. The initial room temperature Raman intensity can be regained approximately by refocusing the laser spot on the new sample surface.

The above observations are particularly instructive in connection to the laser-heated experiments reported in Ref. [5]. There the sample is heated by the laser and a balance between absorbed power and conduction through the gas determines the steady state temperature. If we assume the same temperature induced morphology changes, the amount of absorbed laser power per unit volume is reduced by the defocusing, *i.e.* the reduced laser power-density on the sample. As a result the steady state temperature will not increase in the same manner, and hence the slope in the $\Delta\omega$ vs. laser power plot will change.

Figure 4a shows a low-temperature (2 K) laser power series of Raman spectra at moderate powers below 7 mW. For selected spectra the individual powers are indicated in the plot. The spectra are shifted along the ordinate in order to give a better view. The red vertical line marks the low laser-power Raman peak position of approximately 522.7 cm^{-1} . Surprisingly, although surrounded by superfluid helium, the phonon mode also shifts to lower frequencies in the presented power range. The magnitude of the red-shift at 2 K is smaller than the observed shift in room temperature measurements. In Fig. 4b) the peak positions of a) are plotted against laser power. In the range 0-6.4 mW a red-shift of approximately 3 cm^{-1} is detected. The red line represents the theoretical temperature dependence of the LO phonon mode after Hart *et al.* [11], which considers three phonon processes. We excluded the extension to four phonon processes by Balkanski *et al.* [12] as we are only considering the low temperature limit. To fit our ex-

perimental results we assume proportionality between laser power P and SiNW temperature T . In the limit of T approaching zero we find a lower Raman frequency ω_0 of 525.7 cm^{-1} the main reason is the phonon confinement in our SiNWs [4, 13, 14] leading to a red-shift of approximately 1 cm^{-1} . With this procedure we can now provide a temperature scale to the Raman shift versus laser power plot, which is shown at the top of Fig. 4b).

From a spectroscopic point of view we believe that the temperature at the surface of the SiO shell always remains at $\approx 2 \text{ K}$ (below the lambda point of helium). Due to the large thermal conductivity [15] of superfluid helium the heat dissipated by the SiNWs is effectively removed. A temperature increase to the normal state of helium (occurring at sufficiently higher laser powers) would be visible by gaseous helium bubbles *i.e.* boiling [16]. However, if the temperature at the SiO/He interface is at 2 K , extremely large temperature gradients within the oxide shell and within the silicon core follow. For a rough estimate we calculate the thermal conductivity by evaluating the approximate conducted heat H , which equals the absorbed laser power in thermal equilibrium. By definition of the thermal conductivity K , $H = K \cdot \Delta T$. The thermal conductivity of a SiO cylinder shell is given, in analogy to the electrical, radial resistivity of a cylinder shell by $R = \rho / (2\pi \cdot l) \cdot \ln(r_{\text{outer}}/r_{\text{inner}})$, which is the result of a simple integral and Ohm's law. Here l is the length of the cylinder, r_{inner} and r_{outer} are the inner and outer radii of the cylinder shell, and ρ is the resistivity.

For a laser power of 5 mW we find, according to Fig. 4b, a core temperature of $\approx 250 \text{ K}$. Assuming perfect absorption of the laser light for an upper limit of the thermal conductivity, we find $0.16 \text{ mW}/(\text{K} \cdot \text{m})$. This value is well below the thermal conductivity of fused SiO_2 of $250 \text{ mW}/(\text{K} \cdot \text{m})$ [15] and also lower than the low temperature thermal conductivity of quartz of $\approx 270000 \text{ mW}/(\text{K} \cdot \text{m})$ [15]. These values do not include a possible contact resistance at the solid-liquid He interface, the so called Kapitza resistance [17].

4 Conclusion In conclusion, we investigated the temperature dependence of core-shell SiNWs in a wide temperature range between room temperature and $\approx 900 \text{ K}$, and also at low temperatures (2 K), by means of Raman spectroscopy. Above room temperature we observe a linear dependence showing no signs of a loss of crystallinity. The Raman intensity decreases for increasing temperature indicating gradual changes in sample morphology, explaining saturation effects in laser-heated Raman experiments. Immersed in superfluid helium (at 2 K) SiNWs show a strong build up of heat leading to core temperatures on the order of 300 K .

Acknowledgements ACF acknowledges funding from The Royal Society and The Leverhulme Trust. TEM and SEM images were recorded by D. Berger and U. Gernert in the ZELMI at the TU Berlin.

References

- [1] S. Reich, C. Thomsen, and J. Maultzsch, Carbon Nanotubes: Basic Concepts and Physical Properties (Wiley, New York, 2004).
- [2] Y. W. Son, M. L. Cohen, and S. G. Louie, Nature **444**, 347 (2006).
- [3] R. Gupta, Q. Xiong, C. K. Adu, U. J. Kim, and P. C. Eklund, Nano Lett. **3**, 627 (2003).
- [4] S. Piscanec, M. Cantoro, A. C. Ferrari, J. A. Zapien, Y. Lifshitz, S. T. Lee, S. Hoffmann, and J. Robertson, Phys. Rev. B **68**, 241312(R) (2003).
- [5] H. Scheel, S. Reich, and C. Thomsen, Appl. Phys. Lett. **88**, 233114 (2006).
- [6] A. Colli, A. Fasoli, P. Beecher, P. Servati, S. Pisana, Y. Fu, A. J. Flewitt, W. I. Milne, J. Robertson, C. Ducati, S. De Franceschi, S. Hofmann, A. C. Ferrari, J. Appl. Phys. **102**, 034302 (2007). A. Colli, A. C. Ferrari, S. Hofmann, J. A. Zapien, Y. Lifshitz, S. T. Lee, S. Piscanec, M. Cantoro, and J. Robertson, AIP Conf. Proc. **723**, 445 (2004).
- [7] S. Hofmann, C. Ducati, R. J. Neill, S. Piscanec, A. C. Ferrari, J. Geng, R. E. Dunin-Borkowski, and J. Robertson, J. Appl. Phys. **94**, 6005 (2003).
- [8] C. Thomsen and E. Bustarret, J. Non-Cryst. Solids **141**, 265 (1992).
- [9] J. J. E. Smith, M. H. Brodsky, B. L. Crowder, and M. I. Nathan, Phys. Rev. Lett. **26**, 642 (1971).
- [10] J. Raptis, E. Liarokapis, and E. Anastassakis, Appl. Phys. Lett. **44**, 125 (1983).
- [11] T. R. Hart, R. L. Aggarwal, and B. Lax, Phys. Rev. B **1**, 638 (1970).
- [12] M. Balkanski, R. F. Wallis, and E. Haro, Phys. Rev. B **28**, 1928 (1983).
- [13] I. H. Campbell and P. M. Fauchet, Solid State Commun. **58**, 739 (1986).
- [14] H. Richter, Z. P. Wang, and L. Ley, Solid State Commun. **39**, 625 (1981).
- [15] D. E. Gray (ed.), American Institute of Physics Handbook (Mc Graw-Hill Book Company, 1972).
- [16] W. Dennis, J. E. Durbin, W. A. Fitzsimmons, O. Heybey, and G. K. Walters, Phys. Rev. Lett. **23**, 1083 (1969).
- [17] G. Pollack, Rev. Mod. Phys. **41**, 48 (1969).